

Do biological molecular machines act as Maxwell's demons?

Michał Kurzynski and Przemysław Chelminiak

Faculty of Physics, A. Mickiewicz University, Umultowska 85, 61-614 Poznań, Poland

(Dated: December 7, 2024)

The nanoscopic isothermal machines are not only energy but also information transducers. We show that the generalized fluctuation theorem with information creation and entropy reduction can be fulfilled for the enzymatic molecular machines with the stochastic dynamics, which offers a choice of the work performance in a variety of ways. A specific model of such dynamics is investigated. The main conclusion of the study is that the free energy processing has to be distinguished from the processing of arrangement, which we identify with an adequately defined thermodynamic variable. From the former point of view, Maxwell's demon utilizes entropy reduction ultimately for the performance of work, whereas from the latter, which can be the case of biological molecular machines, only for the creation of information. From a broader biological perspective, three suppositions could be of special importance: (i) a possibility of the choice is characteristic for many intrinsically disordered proteins, (ii) the information creation and storage takes place in the long lasting transient stage before completing the free energy transduction cycle, and (iii) a partial compensation of entropy production by information creation is the reason for most protein machines to operate as dimers or higher organized structures.

PACS numbers: 05.70.Ln, 87.15.H-, 87.15.Ya, 89.75.Hc

INTRODUCTION

In the intention of its creator [1], Maxwell's demon was thought to be an intelligent being, able to perform work at the expense of the entropy reduction of a closed operating system. The perplexing notion of the demons intelligence was formalized in terms of memory and information processing by Szilard [2], Landauer [3] and subsequent followers [4-6], who pointed out that, in order for the total system to obey the second law of thermodynamics, the entropy reduction should be compensated for by, at least, the same entropy increase, related to the demon's information gain on the operating system's state.

The present, almost universal consensus on this issue is expressed in terms of the feedback control [7-12], even if memory has the form of a bit sequence [13-17]. First, information is transferred from the operating system to memory in the process of measurement (observation) and next, when the system is externally loaded, the transfer of information from memory to the operating system controls the work performance process (Fig. 1). Following Landauer's principle, the memory content must be erased at the expense of some entropy production. It should be stressed that the information transfer may [18] but must not be related to energy transfer between the operating system and memory.

A non-informational formulation of the problem was proposed by Smoluchowski [19] and popularized by Feynman [20] as the ratchet and pawl machine. It can operate only in agreement with the second law, at the expense of an external energy source [21]. A. F. Huxley [22] and consequent followers [23, 24] adopted this way of thinking to suggest numerous ratchet mechanisms for the protein molecular machines' action, but no entropy reduction takes place for such models [25], thus, they do

not act as Maxwell's demons. More general models of protein dynamics have been put forward [26-34] with a number of intramolecular states organized in a network of stochastic transitions. Here we show that if such models offer work performance in a variety of ways [34], the generalized fluctuation theorem [7-18, 35-37] is fulfilled with possible entropy reduction. A question appears as to whether they can be considered to act as Maxwell's demons. The hypothetical computer model of the network with the Markovian stochastic dynamics is studied, displaying, like networks of the systems biology [38, 39], a transition from the fractal organization on a small length-scale to the small-world organization on the large length-scale.

We start from the general theory of free energy transduction in mesoscopic isothermal machines and the relationship between the entropy and information produc-

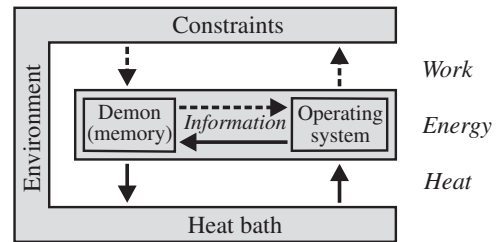


FIG. 1. Feedback control in Maxwell's demon. Entropy reduction (compensated by heat absorption) is related to information creation, but information erasing is related to entropy production (compensated by heat emission). Note that the information transfer must not be described in energy terms so that the operating system and the memory are treated as one energetic unit. When the system is not externally loaded, neither energy nor information is transmitted through the dashed-line arrows.

tion. Then, we present the protein molecular machines as isothermal chemo-chemical machines and state a specific model of the proteins stochastic dynamics. A study of this model, using computer simulations, leads us to the result that the free energy transduction in the fluctuating systems must be distinguished from the arrangement transduction. We identify arrangement with an adequately defined thermodynamic variable and show that its increase, related to an entropy reduction and an information creation, takes place in the transient stage before completing the free energy transduction cycle. The latter, in the case of protein machines, can last quite long. Some biological as well as general physical implications of this statement are the subject of the concluding section.

THEORY: FORMULATION OF THE PROBLEM

Stationary isothermal machines

A long story has been made up for it that the word machine has several different meanings. In our context, we understand a machine to be any physical system that enables two other systems to perform work on one another [40]. The demon considered by Maxwell changed the temperature to perform work at the expense of absorbed heat. However, the biological molecular machines, like the machine considered by Szilard, operate at a constant temperature. Under isothermal conditions, the internal energy is uniquely divided into the free energy, the component that can be turned into work, and the bound energy (the entropy multiplied by the temperature), the component that can be turned into heat. The free energy can be turned irreversibly into the bound energy in the process of internal entropy production, having a meaning of the energy dissipation [41]. In accordance to such internal energy division, the protein molecular machines are referred to as free energy transducers [42], thus, when supposed to act as Maxwells demon, they should perform work at the expense of a part of the dissipation.

During the stationary isothermal processes, both the free energy and the bound energy remain constant. The energy processing pathways in any stationary isothermal machine are shown in Figure 2, where the role of all the physical quantities being in use is also indicated. X_i denotes the input ($i = 1$) and the output ($i = 2$) thermodynamic variable, A_i is the conjugate thermodynamic force and the time derivative, $J_i = dX_i/dt$, is the corresponding flux. T is the temperature and S is the entropy. The thermodynamic variables X_1 and X_2 may be mechanical – displacements, electrical – charges, or chemical – numbers of distinguished molecules, hence the fluxes J_1 and J_2 may be velocities, or electrical or chemical current intensities, respectively. The conjugate forces are then the mechanical forces, or the differences of electrical or chemical potentials (voltages or affinities).

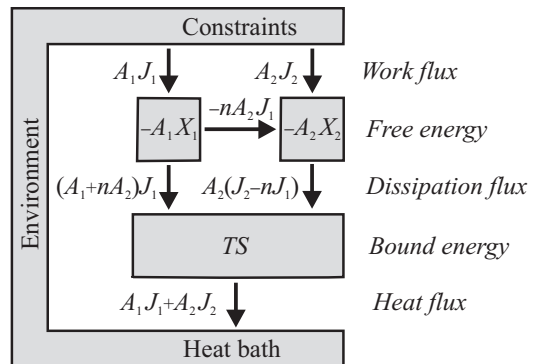


FIG. 2. Energy processing in the stationary (cyclic) isothermal machine. See the text for the explanation. The constraints keep fixed stationary values of the thermodynamic variables X_i . We assume these variables to be dimensionless, hence the conjugate forces A_i are of energy dimension and the fluxes $J_i = dX_i/dt$ are counted in the turnover numbers of the machine per unit time. In a steady state, the work flux (the resultant power) equals the dissipation flux, and that equals the heat flux, which is indicated by the direction of the arrows. The transmission ratio n determines the free energy flux from $-A_1X_1$ to $-A_2X_2$. By convention, the fluxes J_1 and J_2 are assumed to be of the same sign. Then, one system performs work on the other when the forces A_1 and A_2 are of the opposite sign. We assume $J_1, J_2, A_1 > 0$ and $A_2 < 0$ throughout this paper, so that the actual direction of the flux A_2J_2 is in reverse. The actual direction of the flux $A_2(J_2 - nJ_1)$ is the subject of this research.

Machines often work as a gear. To clearly specify the transmission ratio n between the fluxes J_1 and J_2 , determining their tight coupling $J_2 = nJ_1$, it is important that the thermodynamic variables X_1 and X_2 be dimensionless. Then, the fluxes are counted in the turnover numbers of the machine per unit time and the forces are of energy dimension. By convention, the fluxes J_1 and J_2 are assumed to be of the same sign. Then, one system performs work on the other when the forces A_1 and A_2 are of the opposite sign. We assume $J_1, J_2, A_1 > 0$ and $A_2 < 0$ throughout this paper.

According to the second law of thermodynamics, the net dissipation flux (the internal entropy production rate, multiplied by the temperature) $A_1J_1 + A_2J_2$ must be non-negative. However, it consists of two components. The first component, $(A_1 + nA_2)J_1$, achieved when the input and output fluxes are tightly coupled, $J_2 = nJ_1$, and the output energy flux $A_2J_2 = nA_2J_1$ is completely transmitted between the thermodynamic variables X_1 and X_2 (see Figure 2), must also be, according to the same law, nonnegative. Open to discussion is the sign of the complement $A_2(J_2 - nJ_1)$ of $(A_1 + nA_2)J_1$ to the net dissipation flux $A_1J_1 + A_2J_2$.

In the macroscopic systems, the entropy S is additive and can always be divided into the following two parts S_1 and S_2 , relating to the input and output thermodynamic variables X_1 and X_2 , respectively. As a consequence, the

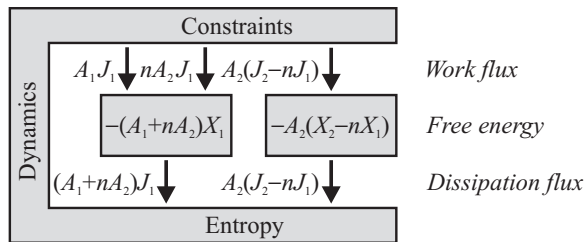


FIG. 3. The alternative view of free energy processing in the stationary isothermal machine. Here, both the thermodynamic variables X_1 and $X_2 - nX_1$ are energetically independent. Only the free energy is specified. The bound energy and the environment are considered to be determined jointly by the dynamics of the machine, modified by an interaction with the environment.

flux $A_2(J_2 - nJ_1)$, which corresponds to S_2 , must also be, under isothermal conditions, nonnegative. This means that, for the assumed negative A_2 , the output flux J_2 should not surpass more than n times the input flux J_1 . Macroscopically, the second component of the dissipation flux has the obvious interpretation of a slippage in the case of the mechanical machines, a short-circuit in the case of the electrical machines, or a leakage in the case of pumps. However, because of non-vanishing correlations within the bound energy subsystem [6 18, 35 37], in the mesoscopic systems like the protein molecular machines, entropy S is not additive and cannot be divided into two parts like the free energy. This allows the transfer of information within the bound energy subsystem, which could result in the partial reduction of energy dissipation.

In fact, for the biological molecular machines, the output flux J_2 can surpass the input flux J_1 [34]. Such a surprising case was observed by Yanagida and his co-workers [43, 44], who found that the single myosin II head can take several steps along the actin filament per ATP molecule hydrolyzed. Whether it changes the sign of the flux $A_2(J_2 - nJ_1)$ to the negative depends on establishing the value of the transmission ratio n , which, as opposed to the macroscopic machines, is not a simple task in the case of molecular machines, and is one of the main topics of the present paper.

From the point of view of the output force A_2 , subsystem 1 carries out work on subsystem 2 while subsystem 2 carries out work on the environment. Jointly, the flux of the resultant work (the resultant power) $A_2(J_2 - nJ_1)$ is driven by the force A_2 . The complement to $A_1J_1 + A_2J_2$ is the flux $(A_1 + nA_2)J_1$ driven by the force $A_1 + nA_2$. Consequently, the free energy processing from Figure 2 can be alternatively presented as in Figure 3, with the free energy transduction path absent. Here, the subsystems described by two variables X_1 and $X_2 - nX_1$, respectively, are energetically independent. However, like the subsystems described by the two variables X_1 and X_2 , they are still statistically correlated. Note that in

Figure 3, only the free energy is specified. The bound energy and the environment are considered as determined jointly by the dynamics of the machine, modified by an interaction with the environment.

Generalized fluctuation theorem

In the mesoscopic machines, the work, dissipation and heat are fluctuating random variables and their variations, proceeding forward and backward in time, are related to each other by the fluctuation theorem [35-37]. In fact, the feedback control description of the Maxwell's demon action [7-18], presented in Figure 1, was based on the fluctuation theorem. For the stationary process, the probability distribution function for the input and output fluxes, in general, depending on the time period t of determination, satisfies the stationary fluctuation theorem in the Andrieux-Gaspard form [45]:

$$\frac{p(j_1(t), j_2(t))}{p(-j_1(t), -j_2(t))} = \exp \beta[A_1j_1(t) + A_2j_2(t)]t. \quad (1)$$

Here, $\beta = 1/k_B T$, where k_B is the Boltzmann constant, and p is the joint probability distribution function for the statistical ensemble of the fluxes $j_1(t)$ and $j_2(t)$ and their inverses. Eq. (1) can be equivalently rewritten as the Jarzynski equality [46]

$$\langle \exp(-\sigma) \rangle = 1 \quad (2)$$

with the stochastic dimensionless entropy production (the energy dissipation divided by $k_B T$)

$$\sigma = \sum_i \beta A_i \mathcal{J}_i(t)t. \quad (3)$$

$\mathcal{J}_i(t)$ in (3) denotes the random variable of the mean net flux over the time period t , ($i = 1, 2$), whereas $j_i(t)$ in (1) denotes its particular value. $\langle \dots \rangle$ is the average over the ensemble of the fluxes $j_1(t)$ and $j_2(t)$. Time t must be long enough for the considered ensemble to comprise only stationary fluxes. The concavity of the exponential function provides the second law of thermodynamics:

$$\langle \sigma \rangle \geq 0 \quad (4)$$

to be a consequence of (2). Only the averages of the random fluxes can be identified with the time-independent stationary fluxes, $\langle \mathcal{J}_i(t) \rangle = J_i$ for arbitrary t .

In further discussion, for brevity, we will omit the argument t specifying all the fluxes. In the context of the transition from Figure 2 to Figure 3, the two-dimensional probability distribution function $p(j_1, j_2)$ can be treated as a two-dimensional probability distribution function of two variables j_1 and $j_2 - nj_1$, with $j_2 - nj_1$ as a whole treated as a single variable. If we calculate the marginal

probability distributions, then, from the fluctuation theorem (1) for the total entropy production in both the stationary fluxes J_1 and J_2 , the generalized fluctuation theorems for J_1 and the difference $J_2 - nJ_1$ follow, respectively, in the logarithmic form:

$$\ln \frac{p(j_1)}{p(-j_1)} = \beta(A_1 + nA_2)j_1 t + \beta A_2 \langle (\mathcal{J}_2 - n\mathcal{J}_1)t \rangle - \left\langle \ln \frac{p(\mathcal{J}_2 - n\mathcal{J}_1 | j_1)}{p(-\mathcal{J}_2 + n\mathcal{J}_1 | -j_1)} \right\rangle \quad (5)$$

(here, the averages $\langle \dots \rangle$ are taken over the ensemble of the flux differences $j_2 - nj_1$) and

$$\ln \frac{p(j_2 - nj_1)}{p(-j_2 + nj_1)} = \beta A_2 (j_2 - nj_1)t + \beta(A_1 + nA_2) \langle \mathcal{J}_1 t \rangle - \left\langle \ln \frac{p(\mathcal{J}_1 | j_2 - nj_1)}{p(-\mathcal{J}_1 | -j_2 + nj_1)} \right\rangle \quad (6)$$

(here, the averages $\langle \dots \rangle$ are taken over the ensemble of the fluxes j_1). Above, we introduced conditional probabilities. The first components on the right of Eqs. (5) and (6) describe the entropy production, now only in the separate fluxes J_1 and $J_2 - nJ_1$, respectively, but the interpretation of the remaining components is not so easy. The problem is that for the stationary processes, as opposed to the transient nonequilibrium protocols considered in Refs. [7-11], the notion of the mutual information is not well defined, as it should be exchanged continuously, without any delay [12].

This disadvantage may, however, be used to determine the value of the transmission ratio n . If it is chosen such that the remaining terms in Eq. (5) cancel each other out and only the entropy production term remains:

$$\ln \frac{p(j_1)}{p(-j_1)} = \beta(A_1 + nA_2)j_1 t \quad (7)$$

then, Eq. (6) for the flux $J_2 - nJ_1$ can be rewritten in terms of the partly averaged mutual information differences:

$$\ln \frac{p(j_2 - nj_1)}{p(-j_2 + nj_1)} = \beta A_2 (j_2 - nj_1)t - \left\langle \ln \frac{p(\mathcal{J}_1, j_2 - nj_1)}{p(\mathcal{J}_1)p(j_2 - nj_1)} \right\rangle + \left\langle \ln \frac{p(-\mathcal{J}_1, -j_2 + nj_1)}{p(-\mathcal{J}_1)p(-j_2 + nj_1)} \right\rangle. \quad (8)$$

Like the antecedent entropic term, both the informative components in Eq. (8) depend only on the single variable $j_2 - nj_1$.

The replacement of (5) by (7) and (6) by (8) is a complete asymmetrical coarse graining [12] of the fluxes J_1 and $J_2 - nJ_1$. This means that J_1 , when averaged over the ensemble of the flux differences $j_2 - nj_1$, is unable to make any choice related to the creation of information, whereas the flux difference $\mathcal{J}_2(t) - n\mathcal{J}_1(t)$, when

averaged over the ensemble of the fluxes j_1 , is able to choose to create some information. In other words, Eq. (7) can be considered as the condition for J_1 to be a hidden thermodynamic variable, from which and to which the information does not flow [14, 15, 47, 48]. The specific value of n results from the internal dynamics of the system; illustrative examples for the biological molecular machines will be presented further on in Figure 5.

To conclude, we write the fluctuation theorem for the flux J_1 , Eq. (7), in the form analogous to the Jarzynski equality (2), from which the second law inequality (4) follows. However, the Jarzynski equality for the flux $J_2 - nJ_1$, Eq. (8), should be written in the generalized form [7-18, 35-37]:

$$\langle \exp(-\sigma - \iota) \rangle = 1 \quad (9)$$

from which the generalized second law inequality follows:

$$\langle \sigma \rangle + \langle \iota \rangle \geq 0 \quad (10)$$

As in Eq. (2), σ has the meaning of the random dimensionless entropy production, while the additional quantity

$$\begin{aligned} \iota = & - \ln \frac{p(\mathcal{J}_1, \mathcal{J}_2 - n\mathcal{J}_1)}{p(\mathcal{J}_1)p(\mathcal{J}_2 - n\mathcal{J}_1)} \\ & + \ln \frac{p(-\mathcal{J}_1, -\mathcal{J}_2 + n\mathcal{J}_1)}{p(-\mathcal{J}_1)p(-\mathcal{J}_2 + n\mathcal{J}_1)} \end{aligned} \quad (11)$$

represents the difference of the stochastic information, which the fluctuating flux $\mathcal{J}_2(t) - n\mathcal{J}_1(t)$ sends outside to the flux $\mathcal{J}_1(t)$, when proceeding, respectively, in the forward and backward directions. Accordingly, $\langle \iota \rangle$ has the direct interpretation of the information production by the flux $J_2 - nJ_1$ and is positive. Because the variable J_1 is hidden this information production is, in fact, the information loss like the entropy production $\langle \sigma \rangle$.

Proteins as chemo-chemical machines

From a theoretical point of view, it is convenient to treat all biological molecular machines as chemo-chemical machines [40]. The protein chemo-chemical machines are enzymes, that simultaneously catalyze two effectively unimolecular reactions: the free energy-donating input reaction $R_1 \leftrightarrow P_1$ and the free energy-accepting output reaction $R_2 \leftrightarrow P_2$ (Fig. 4a). Also, pumps and molecular motors can be treated in the same manner. Indeed, the molecules present on either side of a biological membrane can be considered to occupy different chemical states (Fig. 4b), whereas the external load influences the free energy involved in binding the motor to its track (Fig. 4c), which can be expressed as a change in the effective concentration of this track [27, 28, 33, 34, 40].

The system considered consists of a single enzyme macromolecule, surrounded by a solution of its substrates, possibly involving the track (Fig. 4). It is an

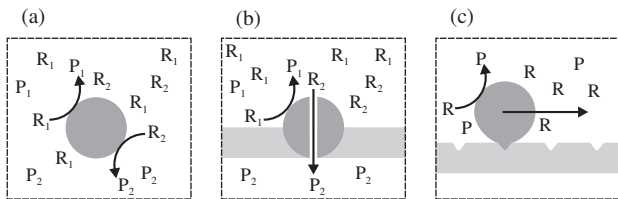


FIG. 4. A simplified representation of the three types of the biological molecular machines: (a) enzymes that simultaneously catalyze two reactions, (b) pumps, and (c) motors. Constraints are symbolized by the frame of the broken line.

open system with constraints controlling the numbers of incoming and outgoing molecules and, in particular, the number of steps performed by the motor along the track. Under specified relations between the concentration of the substrates [34], two independent stationary (nonequilibrium) molar concentrations of the products $[P_1]$ and $[P_2]$, related to the enzyme total concentration $[E]$, are to be treated as the input and output dimensionless thermodynamic variables X_1 and X_2 , respectively, presented in Figure 1. The fluxes J_i with the conjugate thermodynamic forces A_i are determined as [40, 42]

$$J_i \equiv \frac{d}{dt} X_i = \frac{d}{dt} \frac{[P_i]}{[E]}, \quad \beta A_i = \ln \frac{[P_i]^{eq} [R_i]}{[R_i]^{eq} [P_i]} \quad (12)$$

where the superscript eq denotes the corresponding equilibrium concentrations. The fluxes can be calculated if a model of the systems dynamics is at disposal [33, 34].

It is now well established that most if not all enzymatic proteins display slow stochastic dynamics of transitions between a variety of conformational substates composing their native state [49–53]. Two types of experiments imply this statement. The first includes observations of the non-exponential initial stages of a reaction after the special preparation of an initial microscopic state in a statistical ensemble of biomolecules by, e.g., the laser pulse [54, 55]. The second type of experiments is imaging and the manipulation of single biomolecules in various processes [56, 57]. The even more convincing proof of the conformational transition dynamics of native proteins has been provided by molecular dynamics simulations [58, 59]. Here, as a symbol of progress made recently, the study of conformational transitions in intrinsically disordered kinases could be quoted, which a few years ago resulted in a network of 25 substates [60] and now offers a network of several hundred items [61].

To conclude, on the mesoscopic level, the dynamics of a specific biological chemo-chemical machine is the Markov process described by a system of master equations, determining a network of conformational transitions that satisfy the detailed balance condition (we mentioned more representative examples in the Introduction [26–34]), and a system of pairs of distinguished nodes (the gates) between which the input and output chemical reactions force transitions, that break the detailed balance

[33, 34] (Fig. 5a). Recently, we proved analytically [34] that, for a single output gate, when the enzyme has no opportunity for any choice, the ratio $\epsilon = J_2/J_1$ cannot exceed one. This case also includes the various ratchet models [23,24], which assume the output and input gates to coincide. The output flux J_2 can only exceed the input flux J_1 in the case of many output gates, that seems to be the rule rather than the exception [26, 62–66].

At this point, it is worth explaining demonstratively the relationship between the degree of coupling ϵ and the transmission ratio n , which is essential for determining the direction of the flux $A_2(J_2 - nJ_1)$ in Figures 2 and 3. For the assumed negative force A_2 , the sign of $A_2(J_2 - nJ_1) = A_2(\epsilon - n)J_1$ can be negative only if $\epsilon > n$. The value of the degree of coupling ϵ depends, in general, on the values of the forces A_i [33, 34, 40], whereas the specific value of n results from the topology of the network. Two examples of extremely simple networks with two output gates are presented in Figures 5b and c. In the absence of internal transitions indicated by dashed lines, for the gates connected in series, both $n = 2$ and $\epsilon = 2$, independently on the forces A_i , whereas for the gates connected in parallel, both $n = 1$ and $\epsilon = 1$. Consequently, the flux $A_2(J_2 - nJ_1) = A_2(\epsilon - n)J_1$ vanishes in both cases, which is obvious, since there is no short circuit of the input gate that omits the output gates.

The main difference between both examples is that in the one presented in Figure 5b, the system passes along the output gates successively, whereas in the one presented in Figure 5c, it has a choice which output gate

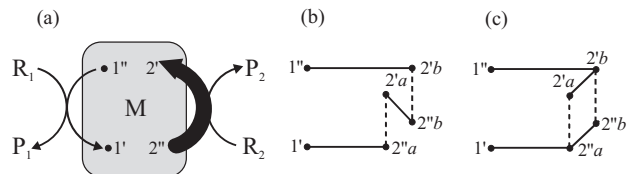


FIG. 5. The kinetics of the enzymatic chemo-chemical machine. (a) General scheme. The grey box represents an arbitrary one-component network of transitions between conformational substates, composing either the enzyme or the enzyme-substrates native state. All these transitions satisfy the detailed balance condition. A single pair (the gate) of conformational states $1''$ and $1'$ is distinguished, between which the input reaction $R_1 \leftrightarrow P_1$ brakes the detailed balance. Also, a single or a variety (the heavy line) of pairs of conformational states $2''$ and $2'$ is distinguished, between which the output reaction $R_2 \leftrightarrow P_2$ does the same. All the reactions are reversible; the arrows indicate the directions assumed to be forward. (b) A simple example of the network of transitions with two output gates connected in series. In the absence of internal transitions indicated by the dashed lines, both the transmission ratio $n = 2$ and the degree of coupling $\epsilon = 2$, otherwise, the latter is lower. (c) The same with two gates connected in parallel. In the absence of internal transitions indicated by the dashed lines, both $n = 1$ and $\epsilon = 1$, otherwise, the latter is lower.

to pass along first. However, by assumption, the network of internal conformational transitions should be one-component, not broken, so that transitions shown by dashed lines must be taken into account. It results in decreasing the value of ϵ [34] and allows the choice of the output gate in both examples. Adding yet other possible transitions changes the value of the transmission ratio n to be established in the whole range from 1 to 2.

Determination of the values of ϵ and n in actual, more complex networks is not a simple task. Our goal in the following is to consider the biological molecular machines with a dynamics with many output gates allowing a choice. Since very poor experimental support is still available for actual conformational transition networks in native proteins, we restrict our attention only to a model network.

METHODS: SPECIFICATION OF THE COMPUTER MODEL

Various models of the networks with several output gates have been considered [34], but one class of models seems to be the most realistic, based on a hypothesis that the protein conformational transition networks, like the higher level biological networks, the protein interaction network and the metabolic network, have evolved in the process of a self-organized criticality [67, 68]. Most networks of the systems biology are scale-free and display a transition from the fractal organization on the small length-scale to the small-world organization on the large length-scale [38, 39].

In Ref. [34], we have shown that the case of many different output gates was reached in a natural way on scale-free fractal trees, extended by long-range shortcuts. A network of 100 nodes with such properties is depicted in Figure 6. The algorithm of constructing the stochastic scale-free fractal trees was adopted after Goh et al. [69]. Shortcuts, though more widely distributed, were considered by Rozenfeld, Song and Makse [38]. Here, we randomly chose three shortcuts from the set of all the pairs of nodes distanced by six links. The network of 100 nodes in Figure 6 is too small to determine its scaling properties, but a similar procedure of construction applied to 10^5 nodes results in a scale-free network, which is fractal on a small length-scale and a small world on a large length-scale. Very recently, a network, which seems to possess similar properties and comprising some 250 nodes, was obtained in a long, 17 μ s molecular dynamics simulation [61].

To provide the network with stochastic dynamics, we assumed the probability of changing a node to any of its neighbors to be the same in each random walking step [34, 70]. Then, following the detailed balance condition, the free energy of a given node is proportional to the number of its links (the node degree). The most stable nodes

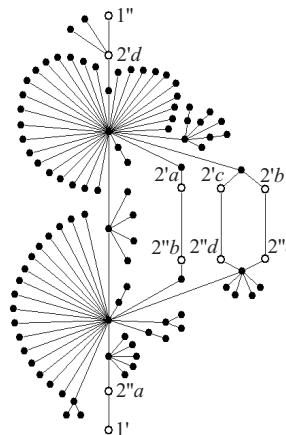


FIG. 6. Exemplifying implementation of the 100-node network, constructed following the algorithm described in Methods. The stochastic dynamics on this network is also described there. Note the two hubs, the states of the lowest free energy, that can be identified with the two main conformations of the protein machine, e.g., open and closed, or bent and straight, usually the only ones occupied sufficiently high to be notable under equilibrium conditions. The single pair of the output transition states (the gate) chosen for the simulations is $(2''a, 2'd)$. The alternative four output pairs $(2''a, 2'a)$, $(2''b, 2'b)$, $(2''c, 2'c)$ and $(2''d, 2'd)$ are chosen tentatively to lie one after another.

are the hubs, which are the only practically observed conformational substates under equilibrium conditions. For a given node l , the transition probability to one of the neighboring nodes is inversely proportional to the number of links, thus to the equilibrium occupation probability p_l^{eq} of the output node, and equals $(p_l^{\text{eq}}\tau_{\text{int}})^{-1}$, where τ_{int} is the mean internal transition time. The latter is determined by the doubled number of links minus one, $\tau_{\text{int}} = 2(100 + 3 - 1) = 204$ random walking steps for the 100 node tree network with 3 shortcuts assumed. To compare, we found the mean first passage time between the most distant nodes to equal 710 random walking steps.

The forward external transition probability, related to the stationary concentration $[P_i]$, is determined by the mean external transition time τ_{ext} , and equals $(p_i^{\text{eq}}\tau_{\text{ext}})^{-1}$ per random walking step, p_i^{eq} denoting the equilibrium occupation probability of the initial input or output node ($i = 1, 2$, respectively). The corresponding backward external transition probability is modified by the detailed balance breaking factors $\exp(-\beta A_i)$. The assumed mean forward external transition time $\tau_{\text{ext}} = 20$ was one order of the magnitude shorter than the mean forward internal transition time $\tau_{\text{int}} = 204$, so that the whole process is controlled by the internal dynamics of the system, not the external. The assumption that most biochemical reactions are controlled by the slow dynamics of the proteins has a very rich literature confirmations [26, 40]. It is this, in fact, that led to the now widely accepted

change of the fundamental paradigm of molecular biology, that not only structure but also dynamics determine the function of the proteins [49-53, 71].

RESULTS

Determination of the transient time

All the averages in the equations from (2) to (10) are to be performed over a statistical ensemble of the stationary fluxes determined for the time period t . We can obtain such an ensemble by dividing a long stochastic trajectory of random walk on the studied network into the segments of the length t , and, next, by determining the net numbers of external transitions, hence, the values of the fluxes $j_1(t)$ and $j_2(t)$ for each segment. However, we have to be sure that the time period t is long enough for the considered ensemble to comprise only stationary, but not transient fluxes.

Because the initial state is random in the successive divisions of the trajectory into the segments of equal length, the averaged value of the flux $\langle \mathcal{J}_i(t) \rangle$ (but not the higher moments!) coincides practically with its stationary value J_i , even for the very short time period t . To evaluate the actual mean transient time t_{tr} , long after which the fluxes become stationary, we have first to divide the whole trajectory into the cycles or protocols [35, 36] of transient trajectories, starting and ending in the same state, say $1'$. For the ensemble of the cycles of the length t , or t within a certain small range, we can determine the time-dependent averages $J_1(t)$ and $J_2(t)$, and in such a way find the time, after which the dynamics of the studied system passes from the transient to the stationary stage.

We performed Monte Carlo simulations of random walk in 10^{10} computer steps on the network shown in Figure 6 with the dynamics specified above, with both the single and the fourfold output gate. The gates were chosen tendentially to maximize the value of the degree of coupling $\epsilon = J_2/J_1$. We assumed $\beta A_1 = 1$ and a few smaller, negative values of βA_2 determining the ratio J_2/J_1 . The presence of external transitions, breaking the detailed balance, makes some computational complications, which are discussed and explained in details elsewhere [70].

The time dependences of the means over cycles $J_1(t)$ and $J_2(t)$, found in our model random walk simulations, will be the subject of a separate paper. Here, only the time dependence of $J_2(t)$ and $J_2(t) - J_1(t)$ for the fourfold output gate and a chosen value of the ratio J_2/J_1 is depicted in Figure 7. We do not present both $J_1(t)$ and $J_2(t)$, because they tend to values completely different from the stationary values J_1 and J_2 , respectively. This means that the latter are determined mainly in the stationary stages of dynamics, not the transient. Only the difference $J_2(t) - J_1(t)$ tends to zero, which is un-

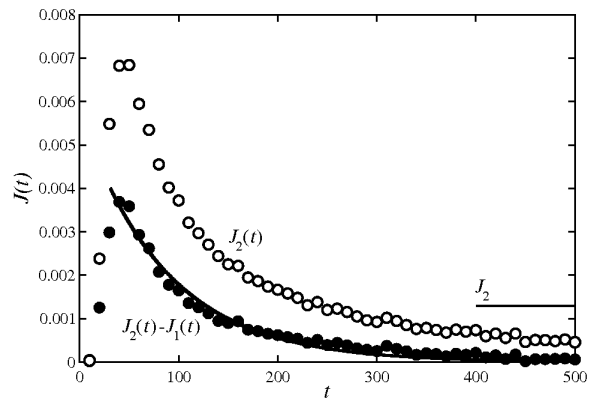


FIG. 7. The time dependence of the averages over cycles $J_2(t)$ and $J_2(t) - J_1(t)$ found in the model random walk simulations on the network shown in Figure 6 with the output gates and the stationary flux ratio $J_2/J_1 = 1.59$. The solid line corresponds to exponential fitting, with $t = 100$ random walking steps, of the flux difference $J_2(t) - J_1(t)$ downfall to zero. The stationary value of $J_2(t)$ is also quoted.

derstandable, because the transition through the input gate each time starts the trajectory from the initial state $1'$ and the whole contribution to the stationary difference $J_2(t) - J_1(t)$ originates from the transient stage of evolution. Exponentially fitting the downfall of the flux difference $J_2(t) - J_1(t)$ to zero allows us to evaluate the transient time value for the case of the fourfold output gate to be approximately $t_{tr} = 100$ random walking steps.

Determination of the transmission ratio

Many trials with divisions of the whole trajectory into segments of different lengths result in the conclusion that

- (i) The obtained two-dimensional probability distribution functions $p(j_1(t), j_2(t))$ actually satisfy the Andrieux-Gaspard fluctuation theorem (1) for t longer than the transient time t_{tr} .

To generate the statistical samples of the stationary fluxes numerous enough, we have chosen the time of the stationary averaging $t = 10^4$ random walking steps for the single gate and $t = 10^3$ random walking steps for the fourfold gate. Exemplary two-dimensional probability distribution functions $p(j_1(t), j_2(t))$ are shown in Figure 8.

We calculated the marginal $p(j_1)$ of the two-dimensional probability distribution functions $p(j_1, j_2)$. Upon analyzing the results, we found that

- (ii) The logarithm of the ratio of the marginals $p(j_1)/p(-j_1)$ can be described by the formula (5) with both the entropic and additional components linearly depending on j_1 . The correction to entropy production is

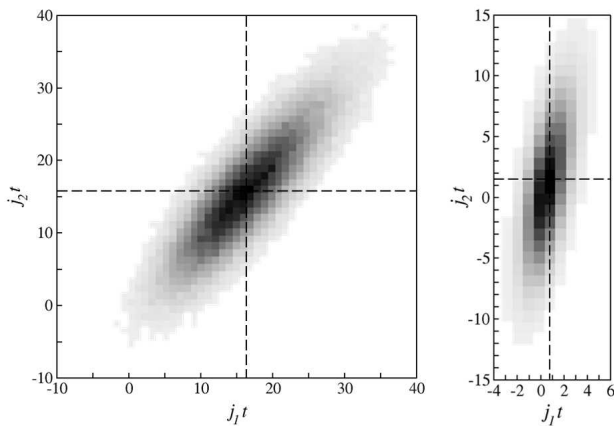


FIG. 8. Exemplifying two-dimensional probability distribution functions $p(j_1(t), j_2(t))$ found in the model random walk simulations on the network shown in Figure 6 with the single output gate (left) and the fourfold output gate (right). For the single output gate, we assumed $t = 10^4$ random walking steps and $J_2/J_1 = 0.95$. For the fourfold output gate, we assumed $t = 10^3$ random walking steps and $J_2/J_1 = 1.59$. See the text for more details. The averaged values of the individual fluxes, multiplied by the time t of the determination, are marked by the dashed lines.

negative.

The dependences of $\ln p(j_1)/p(-j_1)$ on $j_1 t$, when divided by βA_1 , are plotted in Figure 9 and fitting these dependences to Eq. (7) allowed us to determine the value of the transmission ratio to be $n = 1.00$ for the single output gate and $n = 2.27$ for the fourfold output gate.

Knowing the values of n , we determined the marginal distributions $p(j_2 - n j_1)$ of the two-dimensional probability distributions $p(j_1, j_2)$, and found that

(iii) The logarithm of the ratio of the marginals $p(j_2 - n j_1)/p(-j_2 + n j_1)$ can be described by the formula (8) with both the entropic and informative components linearly depending on $j_2 - n j_1$. The informative correction is, as expected, positive.

Exemplary verifications of Eq. (8) are depicted in Figure 10 both for the single (left) and the fourfold (right) output gate. Three markedly different values of the ratio $\epsilon = J_2/J_1$ were chosen for each case. The thick, solid line corresponds to the lack of information production in Eq. (8). Such a case takes place for the force $\beta A_2 = -0.670$, that stalls the flux through the single output gate ($J_2/J_1 = 0$). The same effect of stalling the flux through the fourfold output gate is reached for $\beta A_2 = -0.173$, but this is accompanied by a non-zero information production (the line with a larger slope) resulting from the possibility of the choice of the output gate even if the resultant net flux is zero. The greatest value of the degree of coupling $\epsilon = J_2/J_1$ is reached for

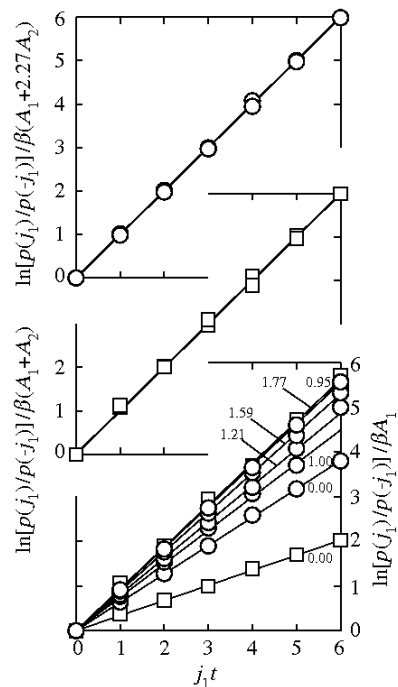


FIG. 9. The generalized fluctuation theorem dependence (5) found in the model random walk simulations. The examined network was the one shown in Figure 6 with the single output gate (the squares) and the fourfold output gate (the circles). We assumed $\beta A_1 = 1$ and a few smaller, negative values of βA_2 determining the ratio $\epsilon = J_2/J_1$ of the average output and input fluxes noted in the figure. At the beginning, the dependence was related to the force βA_1 (the lowest diagram). Relating it to $\beta A_1 + n A_2$, Eq. (7), allowed us to fit the value of the reduction ratio n to be 1.00 for the single output gate (the higher diagram), and 2.27 for the fourfold output gate (the highest diagram). In the last diagram, many simulation points practically cover each other.

$A_2 = 0$, which is represented by the vertical line in both diagrams. It corresponds to $\epsilon = 0.98$ for the single output gate, and $\epsilon = 2.01$ for the fourfold output gate. As a consequence, because of $\epsilon < n$ in both cases, the entropy production rate $\beta A_2(J_2 - n J_1) = \beta A_2(\epsilon - n)J_1$ is always positive. The important conclusion is that the direction of the flux considered in Figures 2 and 3 to be forward or reverse, should always be forward.

Contribution from transient fluxes

The nanoscopic machines are not only energy but also information transducers. In other words, information can serve as a thermodynamic resource similar to free energy there [37, 72]. Up to then, we treated information as an appropriately averaged mutual information exchanged between two subsystems [7-12]. However, it may also be considered as the content of a sequence of bits [13-16] and both the approaches are equivalent [17]. Two types of

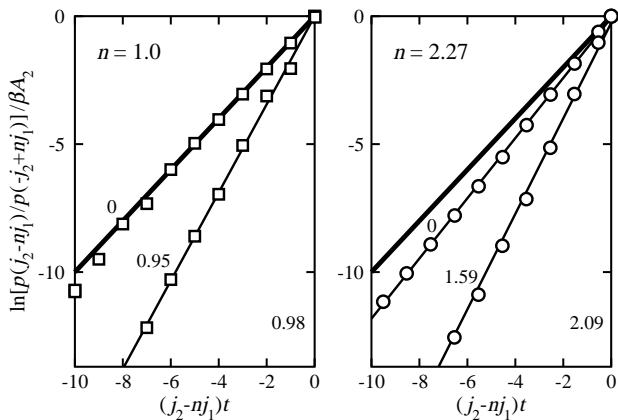


FIG. 10. The generalized fluctuation theorem dependence (8) for the marginal $j_2 - nj_1$, found in the model random walk simulation for the single ($n = 1$, left) and the fourfold ($n = 2.27$, right) output gate. The thick, solid line corresponds to the lack of information production in Eq. (8). Three markedly different values of the ratio $\epsilon = J_2/J_1$ were chosen for each case. Because the corresponding values of βA_2 are negative, the simulation points lie in the lower half-plane of the graph. See the text for more detailed discussion.

information in the second sense are produced during the time course of the simulated process with many output gates. The first is in the form of a string with a more or less random sequence of letters, e.g.

$$\dots b c d d a c b b a b c c \dots$$

labelling successive gates, which the system passed through. And the second is in the form of a string with a more or less random sequence of signs, e.g.

$$\dots + + - + - - + + + \dots$$

describing the directions (forward or backward) of the successive transitions through the output gates.

Nowadays, it is impossible to determine the information of the first type experimentally, and for its theoretical determination, detailed studies of individual, successive transient protocols related to individual trajectories are needed [36, 37]. However, the information of the first type strongly influences information of the second type, directly registered in the single biomolecule experiments [43, 44, 56, 57]. The information of the second type flows out of the machine and defines the number of the product molecules P_2 , hence, the fluctuating variable X_2 .

Both types of information are erased each time the system passes forward through the input gate $1''1'$ and the molecule P_1 is created, hence, the variable X_1 increases by one. In other words, the information created by the molecular machine in the successive transient stages is written in the fluctuating number of product molecules P_2 , created per product molecule P_1 , i.e., in the fluctuating variable $X_2 - X_1$ which differs from the variable

$X_2 - nX_1$ in the case of the multiple output gate. We had already found that the corresponding stationary flux $J_2 - J_1$ is determined entirely by the transient stage dynamics (Fig. 7).

In accordance with the dual interpretation of information [17], also for the flux $J_2 - J_1$, we consider Eq. (6) with $n = 1$ to result in the generalized second law of thermodynamics (10). Formally, upon substituting $n = 1$, the average dimensionless entropy production (the dissipation D divided by $k_B T$) is determined as

$$\beta D \equiv \langle \sigma \rangle = \beta A_2 (J_2 - J_1) t \quad (13)$$

whereas the average information production I , as

$$I \equiv \langle \iota \rangle = \beta (A_1 + A_2) J_1 t \quad (14) \\ - \left\langle \ln \frac{p(\mathcal{J}_1(t) | \mathcal{J}_2(t) - n\mathcal{J}_1(t))}{p(-\mathcal{J}_1(t) | -\mathcal{J}_2(t) + n\mathcal{J}_1(t))} \right\rangle$$

The averages are taken over the joint probability function of the fluxes $p(j_1(t), j_2(t))$.

For the macroscopic machines, there is no correlation between the fluxes, so that only the first term in (14) contributes to the information production I . It indirectly represents the entropy production in the hidden variable X_1 . For the macroscopic machines as well as the mesoscopic enzymatic machines with the single output gate, the information production I and the entropy production βD must always be positive, of the same sign (compare Fig. 10, left). Accordingly, I is to be interpreted as the information loss, like always for any case of the free energy transduction (compare also Fig. 10, right). It is important that for the fourfold output gate and $n = 1$ the difference $J_2 - J_1$ can be positive, thus, for the assumed negative output force βA_2 , the dissipation (13) can be negative, which means the entropy reduction, not the production.

In order to determine the temporal fluctuations of the flux $J_2 - J_1$, we calculated the diagonal marginal $p(j_1 - j_2)$ of the two-dimensional distributions $p(j_1, j_2)$, and found that

(iv) The logarithm of the ratio of the diagonal marginals $p(j_1 - j_2)/p(-j_2 + j_1)$ can be described by the formula (6) with $n = 1$ and all the components linearly depending on the difference $j_2 - j_1$. The informative correction is of the opposite sign to dissipation and large.

The dependences of $\ln p(j_1 - j_2)/p(-j_2 + j_1)$ on $(j_2 - j_1)t$ are depicted in Figure 11 for a few chosen negative values of βA_2 that determine the difference of the averages of the output and input fluxes $J_2 - J_1$, thus, the ratio of those averages $\epsilon = J_2/J_1$. We discarded the rare results for the values of $(j_2 - j_1)t$ higher than 10, as being burdened with a statistical error too large. The simulation data are presented in such a way that the transition from the entropy production to the entropy reduction might be

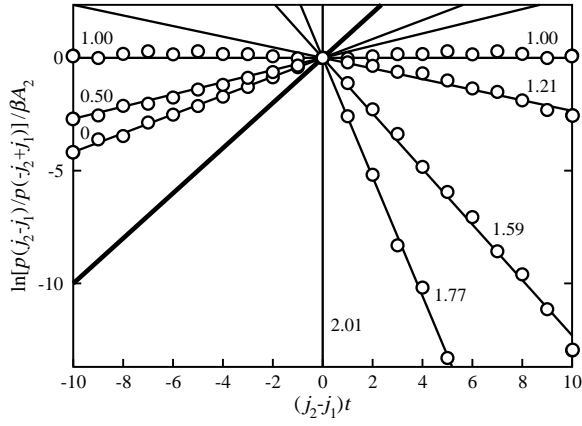


FIG. 11. The generalized fluctuation theorem dependence (6) with $n = 1$, found in the model random walk simulations for the fourfold output gate. The examined network was that shown in Figure 6. We assumed $\beta A_1 = 1$ and a few negative values of βA_2 determining the difference $J_2 - J_1$ of the stationary output and input fluxes (or the degree of coupling $\epsilon = J_2/J_1$ noted in the figure). The results of each simulation were obtained symmetrically on the whole axis of the fluctuating difference $(j_2 - j_1)t$ but in the figure, they are presented, divided by the (negative!) coefficient βA_2 , only on the left from zero for the negative average $J_2 - J_1$, and on the right from zero for the positive average $J_2 - J_1$. The thick, solid line corresponds to the first, entropic component to the right-hand side of Eq. (6). For the multiple output gate, the information gain, resulting from the possibility of a choice, surpasses the information loss in favor of the flux J_1 , and reduces the effects of the entropy production in part, until the limit of $J_2 - J_1 = 0$ ($J_2/J_1 = 1$), above which information production prevails.

clearly seen. The thick, solid line corresponds to the first, entropic term to the right-hand side of Eq. (6). For many output gates, as opposed to the case of a single output gate, the information gain, resulting from the possibility of a choice, surpasses the information loss and reduces the effects of the entropy production in part, until the limit of $J_2 - J_1 = 0$ ($J_2/J_1 = 1$), above which information production prevails.

The stationary values of J_1 and J_2 are unambiguously related to the forces A_1 and A_2 , so we can directly determine the average entropy production (13) for the given time period t . Figure 11 clearly shows the linear relation

$$\beta D + I = \alpha \beta D \quad (15)$$

where α is the tangent of the adequate straight line slope. From (15), knowing βD and α , we can determine the average information production I without referring to the much more complex formula (14). The values of I and βD , obtained from the values of α found from Figure 11, are presented in Figure 12 as the functions of $J_2 - J_1$. Note that for $J_2 - J_1 > 0$, the negative entropy production βD is associated with the positive information production I , which should now be referred to as actual

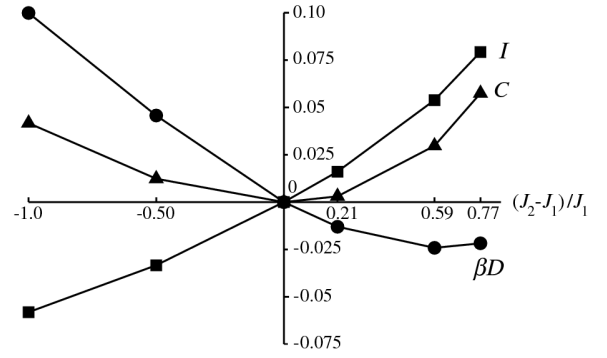


FIG. 12. The dependence of the information production I (the squares) and the entropy production βD (the circles) per $t = 10^3$ random walking steps of determination, on the flux difference $J_2 - J_1$. The points represent the values obtained from the data given in Figure 11. The sum of βD and I , we refer to as the cost C of information processing (the triangles), is also shown.

information creation.

DISCUSSION: FREE ENERGY VERSUS ARRANGEMENT PROCESSING

We have studied the fluctuations of the flux difference $J_2 - J_1$, which is the time derivative of the variable $X_2 - X_1$. This variable characterizes not energy but the degree of arrangement of the system. In the case of the macroscopic mechanical machines, it could be, for example, the possibly slipping angle of a component wheel to the axle. In the case of the macroscopic battery (the electrochemical machine), it is the difference between the available electric charge and the unused amount of reductor, both quantities being determined in molecular units. The arrangement $X_2 - X_1$ is controlled by force A_2 . The arrangement of the macroscopic machines always decreases: the wheels slide with respect to the axles, the batteries wear out. This need not be the case of the fluctuating mesoscopic machines.

The main result of our study is that the free energy processing has to be distinguished from the arrangement processing, which is schematically illustrated in Figure 13. Note that both free energy F and arrangement X are functions of the state of the system. As in Figure 3, the bound energy and the environment are considered to be determined jointly by the dynamics of the machine modified by an interaction with the environment. In the case of the purely stochastic dynamics, the presence of the thermal bath influences the probabilities of the internal transitions, whereas the constraints influence the probabilities of the external transitions. Note that we do not distinguish the operating system and the memory as the previous investigators [7-12] did after the Szilard understanding of Maxwells demon [2]. Rather, as in the

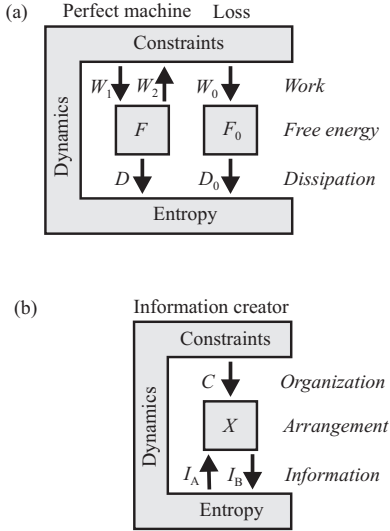


FIG. 13. Free energy (a) versus arrangement (b) processing in the system participating in a stationary isothermal process. The actual directions of the input and output work as well as the input and output information are indicated. As in Figure 3, the bound energy and the environment are considered to be determined jointly by the internal dynamics of the system, modified by an interaction with the environment. See the text for more detailed discussion.

information thermodynamics [72-78], we treat the memory, contained in the internal dynamics of the machine, which determines its entropy, on an equal footing with the constraints.

For the systems operating under isothermal conditions, the first and second laws of thermodynamics:

$$W_1 + W_2 - \Delta F = D \geq 0, \quad W_0 - \Delta F_0 = D_0 \geq 0 \quad (16)$$

are fulfilled for the perfect free energy processing and loss, respectively. For the stationary processes, the free energies F and F_0 remain constant, $\Delta F = \Delta F_0 = 0$. All the components of work W_1 , W_2 , and W_0 , and dissipation D and D_0 are functions of the process. The individual components of Eq. (16), which have been considered in our study, are specified in Figure 3. Loss in the free energy processing means that no work on the environment is performed despite the forced energy dissipation. We have proven that it occurs simultaneously with the information loss for any case of the free energy transduction. In the perfect machine, the output flux is tightly coupled to the input flux, $J_2 = nJ_1$, and the output work is maximum. Dissipation D tends to zero when the perfect stationary machine works infinitely slowly, $J_1 \rightarrow 0$, but, then, its input and output powers also drop to zero.

For the arrangement processing, the generalized first and second law can be written as

$$I_A + I_B - \Delta X = C \geq 0 \quad (17)$$

In our study, arrangement X equals the difference $X_2 - X_1$ and under stationary conditions, it remains constant,

$\Delta X = 0$. Here, the two components of the generalized second law (10), given by Eqs. (13) and (14), are more generally treated as the two components of information: the input one $I_A = \beta D$ and the output one $I_B = I$, respectively. Both I_A and I_B as well as C , the quantity which balances two former quantities and which could be referred to as the organization cost of arrangement, are functions of the process.

All three changes of arrangement in Eq. (17) are in fact the three types of information and are associated with the three strings of bits. When presenting results of our simulations, we described two signals. The first, in the form of a string of letters, corresponds to the organization of arrangement, whereas the second, in the form of a string of signs, corresponds to the information actual. We did not mention the third signal originating in the random number generator, which simulates a noise corresponding to entropy production.

Only the free energy transducer, for which the works W_1 and W_2 are of the opposite sign, can be referred to as the machine. Similarly, only the arrangement transducer, for which the information production I_B and the entropy production I_A are of the opposite sign, can be referred to as the information creator. For I_B being positive, I_A must be negative (the entropy reduction instead of production). The biological molecular machines, for which this is the case, may be said to act as Maxwells demons, although they do not utilize the information creation for the performance of work.

When considering the coupling of the free energy donating process with the free energy accepting one, the case of the tight coupling $J_2 = J_1$ with the reduction ratio $n = 1$, is exceptional. Our simulation clearly points out that for $n > 1$, the case of $J_2 - J_1 = 0$ occurs for the total compensation of entropy reduction I_A by information creation I_B , albeit, on average, both then tend to zero (compare Figure 12). This case is the optimum in the sense that the organization cost C of the total process is then zero.

CONCLUSION

The two powerful theoretical physics tools created at the turn of the century, the fluctuation theorem [35, 36] and the idea of self-organized criticality [67, 68], force a significant change in our views on the nature of the biological molecular machines action. Progress in the theory coincides with the intensive experimental and numerical studies of protein dynamics [49-61]. A possible proposal, not to be underestimated, is that the biological structural memory, traditionally associated with DNA and RNA, can be complemented by a dynamical memory of proteins.

Under the physiological conditions, the protein molecular machines fluctuate constantly between lots of con-

formational substates composing their native state. The probabilities of visiting individual substates are far from equilibrium and determined by the varying concentration of the substrate molecules surrounding the machine. The machine can be considered as an enzyme that simultaneously catalyzes two reactions: the free energy-donating and free energy-accepting ones. During the transient stages between the subsequent free energy transduction cycles, the numerous accomplishments of the free energy-accepting reaction force transitions between separate regions of the conformational substates of the protein machine, which brakes ergodicity [79] of its dynamics until the subsequent free energy-donating reaction takes place. The machine transduces information about the types of successive transitions on the information about their successive directions. In this transduction the third signal can be utilized. It is the purely random noise of the environment. Information about the direction of the successive transitions during the transient stage of the free energy transduction cycle determines the varying difference of the concentrations of the free-energy-accepting and free-energy-donating molecules, surrounding the machine. This difference is a thermodynamic measure of the molecular machines dynamical arrangement and can be the source of information passed to a further use.

The transient dynamics stages during the succeeding free energy transduction cycles can last quite long [61, 80, 81], especially when more shortcuts and external transitions in the conformational transition network are taken into account [71]. Projection of the trajectory on the thermodynamic arrangement variable has a form of time series representing continuous time random walk [61, 80, 81]. It is very likely, that the natively disordered transcription factors, in their one-dimensional search for the target intermittent by three-dimensional flights [82, 83], perform not the passive diffusion but the active continuous time random walk.

As mentioned earlier [34], our approach is able to explain the observation, that the single myosin II head can take several steps along the actin filament per ATP molecule hydrolyzed [43, 44]. It is likely that the mechanism of the action of the small G-proteins such as Ras, which have a common ancestor with the myosin [84] and an alike partly disordered structure after binding the nucleoside triphosphate [85-87], is, after a malignant transformation, similar. Of course, we cannot claim that the model considered here has something to do with the dynamics of the myosin had or the small G-proteins, but in future, a more adequate model is worth considering.

In the healthy cells, the G-proteins play the role of signal transducers that activate various kinases, which further transmit the signal to the target. The chemotactic response of *Escherichia coli* to methylation of a receptor, leading to activation of the flagellar motor to move, is a relatively simple experimental model investigated in more detail [88]. Theory of the biochemical signal trans-

duction in this system is the subject of intensive research [72-78]. Here, the information is also stored in the form of the concentration of specific molecules like in the system considered in the present paper. It would be interesting to combine both approaches.

There are some arguments, for instance, for the kinesin motor [89-93], the myosin V motor [94], the cytoplasmic dynein motor [95,96], the quinol:cytochrome c oxidoreductase [97,98], and the very Ras molecules [99,100] that a feedback control with the tight coupling, $J_2 = J_1$, is achieved in dimeric protein complexes, which are composed of two identical monomers. We have ascertained that the case of the total compensation of the entropy production by information creation is the optimum in the sense that the cost of the total process is then zero. This may occur for a binary system, whose components create and collect information alternately in such a way that the resultant information and entropy productions are zero. The cyclic, alternate behavior is important for the corresponding cost in the stationary process could not be assigned to individual components. In this respect, the corresponding models should differ essentially from those of the bipartite systems [11, 12], and are worth a separate study. Research of this kind could help to answer the certainly interesting question: why do most protein machines operate as dimers or higher organized structures?

The main conclusion of the paper is that the free energy processing has to be distinguished from the arrangement processing. From the former point of view, Maxwell's demon utilizes entropy reduction ultimately for the performance of work, whereas from the latter, only for the creation of information. Our answer to the question posed in the title is that the biological molecular machines can, under certain conditions, act as Maxwell's demons, but only creating information, and not performing work. This statement is based on the relationship $\epsilon < n$ between the degree of coupling ϵ and the transmission ratio n shown to hold for the studied model of dynamics. There is still the need to prove the generality of this relationship.

We know that work, heat and dissipation (the entropy production) are changes of energy. But there is still controversy, the change of which physical quantity is information [101]? Here, we suggest the answer that information is the change of arrangement, a quantity being the difference of two physical quantities X_2 and X_1 taking part in the free energy-transduction process and describing the free energy reception and delivery, respectively. In such an approach, the dual nature of entropy becomes clear as the physical quantity that connects the processes of free energy and arrangement transduction.

At the end, let us take the liberty for a couple of speculation. The first and second laws of thermodynamics (16) are valid for any isothermal processes, whereas the suggested first and second laws of arrangement transduc-

tion (17) were justified only for the stationary isothermal processes. The open problem remains the generality of these laws. One thing is certain: the necessary conditions for the information and entropy productions to be of the opposite signs, is the presence of fluctuations and the possibility of a choice. Besides the mesoscopic machines, we know three macroscopic systems sharing such properties and intriguing long. The first and the best known are the systems with critical thermodynamic fluctuations, whose arrangement is determined by new long-living thermodynamic variables that survives stochasticization [102], referred to as the order parameters [41] or, in various contexts, emergent [103] or structural [40] variables. The second are the systems displaying quantum fluctuations entangled with the environment, whose arrangement is determined by classical variables that survives decoherence [104,105]. And the third, living systems display a non-gradual stochastic Darwinian evolution, and their arrangement is determined by the survival degree of species, resistant against mutations [106,107].

Acknowledgements. MK thanks Yasar Demirel and Herve Cailleau for discussing the problem in the early stages of the investigation.

Author Contributions. The general concept and the theory is mainly due to MK, who also wrote the manuscript. The specification of the critical branching tree model and the numerical simulations are mainly due to PC.

Conflict of Interest. None declared.

-
- [1] Maxwell, J. C. Theory of Heat (Logmans, London, 1871).
- [2] Szilard, L. Z. On the decrease of entropy in a thermodynamic system by the intervention of intelligent beings. *Z. Phys.* 53, 840-857 (1929).
- [3] Landauer, R. Irreversibility and heat generation in the computing process. *IBM J. Res. Dev.* 5, 183-191 (1961).
- [4] Leef, H. S. & Rex, E. eds., *Maxwell's Demon 2: Entropy, Classical and Quantum Information, Computing* (Institute of Physics Publishing, Philadelphia, 2003).
- [5] Maruyama, K., Nori, F. & Verdal, V. Colloquium: The physics of Maxwell's demon and information. *Revs. Mod. Phys.* 81, 1-23 (2009).
- [6] Sagawa, T. *Thermodynamics of Information Processing in Small Systems* (Springer, Berlin, 2013).
- [7] Sagawa, T. & M. Ueda, M. Generalized Jarzynski equality under nonequilibrium feedback control. *Phys. Rev. Lett.* 104, 090602 (2010).
- [8] Ponnuragan, M. Generalized detailed fluctuation theorem under nonequilibrium feedback control. *Phys. Rev. E* 82, 031129 (2010).
- [9] Sagawa, T. & Ueda, M. Nonequilibrium thermodynamics of feedback control. *Phys. Rev. E* 85, 021104 (2012).
- [10] Sagawa, T. & Ueda, M. Role of mutual information in entropy production under information exchanges. *New J. Phys.* 15, 125012 (2013).
- [11] Hartich, D., Barato, A. C. & Seifert, U. Stochastic thermodynamics of bipartite systems: transfer entropy inequalities and a Maxwell's demon interpretation. *J. Stat. Mech.* 14, P02016 (2014).
- [12] Horowitz, J. M. & Esposito, M. Thermodynamics with continuous information flow. *Phys. Rev. X* 4, 031015 (2014).
- [13] Mandal, D. & Jarzynski, C. Work and information processing in a solvable model of Maxwell's demon. *Proc. Natl. Acad. Sci. USA* 109, 11641-11645 (2012).
- [14] Barato, A. C. & Seifert, U. Stochastic thermodynamics with information reservoirs. *Phys. Rev. Lett.* 112, 090601 (2014).
- [15] Shiraishi, N. & Sagawa, T. Fluctuation theorem for partially masked nonequilibrium dynamics. *Phys. Rev. E* 91, 012130 (2015).
- [16] Shiraishi, N., Ito, S., Kawaguchi, K. & Sagawa, T. Role of measurement-feedback separation in autonomous Maxwell's demons. *New J. Phys.* 17, 045012 (2015).
- [17] Shiraishi, N., Matsumoto, T. & Sagawa, T. Measurement-feedback formalism meets information reservoirs. *New J. Phys.* 18, 013044 (2016).
- [18] Deffner, S. & Jarzynski, C. Information processing and the second law of thermodynamics: An inclusive, Hamiltonian approach. *Phys. Rev. X* 3, 041003 (2013).
- [19] Smoluchowski, M. Experimentell nachweisbare der ueblichen Thermodynamik widersprechende Molekulaphaenomene. *Phys. Z.* 13, 1069-1080 (1912).
- [20] Feynman, R. P., Leighton, R. B. & Sands, M. *The Feynman Lectures on Physics*, vol. 1, chap. 46 (Addison-Wesley, Reading, 1963).
- [21] Jarzynski, C. & Mazonka, O. Feynman's ratchet and pawl: An exactly solvable model. *Phys. Rev. E* 59, 6448-6459 (1999).
- [22] Huxley, A. F. Muscle structure and theories of contraction. *Prog. Biophys. Biophys. Chem.* 7, 255-318 (1957).
- [23] Howard, J. *Mechanics of Motor Proteins and the Cytoskeleton* (Sinauer, Sunderland, 2001).
- [24] Howard, J. Motor proteins as nanomachines: the roles of thermal fluctuations in generating force and motion. In *Biological Physics - Poincare Seminar 2009*, Duplainer, B. & Rivasseau, V., eds, pp. 47-60 (Springer, Basel, 2010).
- [25] Horowitz, J. M., Sagawa, T. & Parrondo, J. M. R. Imitating chemical motors with optimal information motors. *Phys. Rev. Lett.* 111, 010602 (2013).
- [26] Kurzynski, M. A synthetic picture of intramolecular dynamics of proteins. Towards a contemporary statistical theory of biochemical processes. *Prog. Biophys. Molec. Biol.* 69, 23-82 (1998).
- [27] Fisher, M. A. & Kolomeisky, A. B. The force exerted by a molecular motors. *Proc. Natl. Acad. Sci. USA* 96, 6597-6602 (1999).
- [28] Kolomeisky, A. B. & Fisher, M. E. Molecular motors: A theorist's perspective. *Annu. Rev. Phys. Chem.* 58, 675-95 (2007).
- [29] Astumian, R. D. & Derenyi, I. A chemically reversible Brownian motor: Application to kinesin and Ncd. *Biophys. J.* 77, 993-1002 (1999).
- [30] Bustamante, C., Keller, D. & Oster, G. The physics of molecular motors. *Acc. Chem. Res.* 34, 412-420 (2001).
- [31] Lipowsky, R. Universal aspects of the chemomechanics

- cal coupling for molecular motors. *Phys. Rev. Lett.* 85, 4401-4406 (2000).
- [32] Lipowsky R., Liepelt, S. & Valleriani, A. Energy conversion by molecular motors coupled to nucleotide hydrolysis. *J. Stat. Phys.* 135, 951-275 (2009).
- [33] Kurzynski, M. & Chelminiak, P. Mean first-passage time in stochastic theory of biochemical processes. Application to actomyosin molecular motor. *J. Stat. Phys.* 110, 137-181 (2003).
- [34] Kurzynski, M., Torchala, M. & Chelminiak, P. Output-input ratio in thermally fluctuating biomolecular machines. *Phys. Rev. E* 89, 012722 (2014).
- [35] Jarzynski, C. Equalities and inequalities: Irreversibility and the second law of thermodynamics at the nanoscale. *Annu. Rev. Condens. Matter Phys.* 2, 329-351 (2011).
- [36] Seifert, U. Stochastic thermodynamics, fluctuation theorems and molecular machines. *Rep. Prog. Phys.* 75, 126001 (58pp) (2012).
- [37] Parrondo, J. M. R., Horowitz, J. M. & Sagawa, T. Thermodynamics of information. *Nature Phys.* 11, 131-139 (2015).
- [38] Rozenfeld, H. D., Song, C. & Makse, H. A. Small-world to fractal transition in complex networks: A renormalization group approach. *Phys. Rev. Lett.* 104, 025701 (2010).
- [39] Escolano, F., Handcock, E. R. & Lozano, M. A. Heat diffusion: Thermodynamic depth complexity of networks. *Phys. Rev. E* 85, 036206 (2012).
- [40] Kurzynski, M. *The Thermodynamic Machinery of Life* (Springer, Berlin, 2006).
- [41] Callen, H. B. *Thermodynamics and an Introduction to Thermostatistics* 2nd edn. (Wiley, New York, 1985).
- [42] Hill, T. L. *Free Energy Transduction and Biochemical Cycle Kinetics* (Springer, New York, 1989).
- [43] Kitamura, K., Tokunaga, M., Iwane, A. H. & Yanagida, T. A single myosin head moves along an actin filament with regular steps of 5.3 nanometers. *Nature* 397, 129-134 (1997).
- [44] Kitamura, K., Tokunaga, M., Esaki, S., Iwane, A. H. & Yanagida, T. Mechanism of muscle contraction based on stochastic properties of single actomyosin motors observed in vitro. *Biophysics* 1, 1-19 (2005).
- [45] Andrieux, D. & Gaspard, P. Fluctuation theorem for currents and Schnakenberg network theory. *J. Stat. Phys.* 127, 107 (2007).
- [46] Jarzynski, C. Nonequilibrium equality for free energy differences. *Phys. Rev. Lett.* 78, 2690-2693 (1997).
- [47] Mehl, J., Lander, B., Bechinger, C., Blickle, V. & Seifert, U. Role of hidden slow degrees of freedom in the fluctuation theorem. *Phys. Rev. Lett.* 108, 220601 (2012).
- [48] Borrelli, M., Koski, J. V., Maniscalco, S. & Pekola, J. P. Fluctuation relations for driven coupled classical two-level systems with incomplete measurements. *Phys. Rev. E* 91, 012145 (2015).
- [49] Henzler-Wildman, K. & D. Kern, D. Dynamic personalities of proteins. *Nature* 450, 964-972 (2007).
- [50] Uversky, V. N. & Dunker, A. K. Understanding protein non-folding. *Biochim. Biophys. Acta* 1804, 1231-1263 (2010).
- [51] Chouard, D. Breaking the protein rules. *Nature* 471, 151-153 (2011).
- [52] Chodera, J. D. & Noe, F. Markov state models of biomolecular conformational dynamics. *Curr. Opin. Struct. Biol.* 25, 135-144 (2014).
- [53] Shukla, D., Harnandez, C. X., Weber, J. K. & Pande, V. S. Markov state models provide insight into dynamic modulation of protein function. *Acc. Chem. Res.* 48, 414-422 (2015).
- [54] Austin, R. H., Beeson, K. W., Eisenstein, L., Frauenfelder, H. & Gunsalus, I. C. Dynamics of ligand binding to myoglobin. *Biochemistry* 14, 5355-5373 (1975).
- [55] Frauenfelder, H. *The Physics of Proteins: An Introduction to Biological Physics and Molecular Biophysics* (Springer, Berlin, 2010).
- [56] Ishijima, A. & Yanagida, T. Single molecule nanobiology. *Trends Biochem. Sci.* 26, 438-444 (2001).
- [57] Yanagida, T. & Ishii, Y., eds. *Single Molecule Dynamics in Life Science* (Wiley-VCH, Weinheim, 2008).
- [58] Kitao, A., Hayward, S. & Go, N. Energy landscape of a native protein: Jumping-among-minima model. *Proteins* 33, 496-517 (1998).
- [59] Karplus, M. & McCammon, J. A. Molecular dynamics simulations of biomolecules. *Nature Struct. Biol.* 9, 646-52 (2002).
- [60] Yang, S., Banavali, N. K. & Roux, B. Mapping the conformational transitions in Src activation by cumulating the information from multiple molecular dynamics trajectories. *Proc. Natl. Acad. Sci. USA.* 106, 3776-3781 (2009).
- [61] Hu, X., Hong, L., Smith, M. D., Neusius, T., Cheng, X. & Smith, J. C. The dynamics of single protein molecules in non-equilibrium and self-similar over thirteen decades in time. *Nature Phys.* 12, 171-174 (2016).
- [62] Zwanzig, R. Rate processes with dynamical disorder. *Acc. Chem. Res.* 23, 148-152 (1990).
- [63] Lu, H. P., Xun, L. & Xie, X. S. Single-molecule enzymatic dynamics. *Science* 282, 1877-1882 (1998).
- [64] English, B. P., Min, W., van Oijen, A. M., Lee, K. T., Luo, G. & Sun, H., et al. Ever-fluctuating single enzyme molecules: Michaelis-Menten equation revisited. *Nature Chem. Biol.* 2, 87-94 (2006).
- [65] Kurzynski, M. Statistical properties of the dichotomous noise generated in biochemical processes. *Cell. Mol. Biol. Lett.* 13, 502-513 (2008).
- [66] Xie, X. S. Enzymatic kinetics, past and present. *Science* 342, 1457-1459 (2013).
- [67] Bak, P. *How Nature Works* (Springer, New York, 1996).
- [68] Sneppen, K. & Zocchi, G. *Physics in Molecular Biology* (Cambridge University Press, New York, 2005).
- [69] Goh, K.I., Salvi, G., Kahng, B. & Kim, D. Skeleton and fractal scaling in complex networks. *Phys. Rev. Lett.* 96, 018701 (2006).
- [70] Chelminiak, P. & Kurzynski, M. Steady-state distributions of probability fluxes on complex networks. *Physica A* 468, 540-551 (2017).
- [71] Kurzynski, M. & Chelminiak, P. Stochastic dynamics of proteins and the action of biological molecular machines. *Entropy* 16, 1969-1982 (2014).
- [72] Ito, S. & Sagawa, T. Information thermodynamics on causal networks. *Phys. Rev. Lett.* 111, 180603 (2013).
- [73] Barato, A. C., Hartrich, D. & Seifert, U. Information-theoretic versus thermodynamic entropy production in autonomous sensory networks. *Phys. Rev. E* 87, 042104 (2013).
- [74] Barato, A. C., Hartrich, D. & Seifert, U. Efficiency of cellular information processing. *New J. Phys.* 16, 103024 (2014).

- [75] Sartori, P., Granger, L., Lee, C. F. & Horowitz, J. M. Thermodynamic cost of information processing in sensory adaptation. *PLOS Comput. Biol.* 10, e1003974 (2014).
- [76] Ito, S. & Sagawa, T. Maxwell's demon in biochemical signal transduction with feedback loop. *Nature Commun.* 6, 2-6 (2015).
- [77] Bo, S., Del Giudice, M. & Celani, A. Thermodynamic limits to information harvesting by sensory systems. *J. Stat. Mech.* (2015) P01014.
- [78] Hartrich, D., Barato, A. C. & Seifert, U. Sensory capacity: An information theoretical measure of the performance of a sensor. *Phys. Rev. E* 93, 022116 (2016).
- [79] Palmer, R. G. Broken ergodicity. *Adv. Phys.* 31, 669-783 (1982).
- [80] Metzler, R. Forever ageing. *Nature Phys.* 12, 113-114 (2016).
- [81] Metzler, R., Jeon, J.-H., Cherstvy, A. G. & Barkai, E. Anomalous diffusion models and their properties: Non-stationarity, non-ergodicity, and aging at the centenary of single particle tracking. *Phys. Chem. Chem. Phys.* 16, 24128-24164 (2014).
- [82] Tafvizi, A., Huang, F., Ferhst, A. R., Mirny, L. A. & van Oijen, A. M. A. A single molecule characterization of p53 search on DNA. *Proc. Natl. Acad. Sci. USA* 108, 263-568 (2011).
- [83] Li, G.-W. & Xie, X. S. Central dogma at the single-molecule levels in living cells. *Nature* 475, 308-315 (2011).
- [84] Kull, F. J., Vale, R. D. & Fletterick, R. J. The case for a common ancestor: kinesin and myosin motor proteins and G proteins. *J. Muscle Res. Cell Motil.* 19, 877-886 (1998).
- [85] Houdusse, A. & Sweeney, H. L. Myosin motors: missing structures and hidden springs. *Curr. Res. Struct. Biology.* 11, 182-194 (2001).
- [86] Kosztin, I., Bruinsma, R., O'Lague, P. & Schulten, K. Mechanical force generation by G proteins, *Proc. Natl. Acad. Sci. USA* 99, 3575-3580 (2002).
- [87] Arai, Y., Iwane, A. H., Wazawa, T., Yokota, T., Ishii, Y., Kataoka, T. & Yanagida, T. Dynamic polymorphism of Ras observed in single molecule FRET is the basis for molecular recognition. *Biochem. Biophys. Res. Commun.* 343, 809-815 (2006).
- [88] Tu, Y., Shimizu, T. S. & Berg, H. C. Modeling the chemotactic response of *Escherichia coli* to time-varying stimuli. *Proc. Natl. Acad. Sci. USA* 105, 14855-14860 (2008).
- [89] Taniguchi, Y., Karagiannis, P., Nishiyama, M., Ishii, Y. & Yanagida, T. Single molecule thermodynamics in biological motors. *BioSystems* 88, 283-292 (2007).
- [90] Bier, M. The stepping motor protein as a feedback control ratchet. *BioSystems* 88, 301-307 (2007).
- [91] Astumian, R. D. Symmetry based mechanism for hand-over-hand molecular motors. *Biosystems* 93, 8-15 (2007).
- [92] Liepelt, S. & Lipowsky, R. Operation modes of the molecular motor kinesin. *Phys. Rev. E* 79, 011917 (2009).
- [93] Astumian, R. D. Thermodynamics and kinetics of molecular motors. *Biophys. J.* 98, 2401-2409 (2010).
- [94] Nishikawa, M., Takai, H., Shibata, T., Ivane, A. F. & Yanagida, T. Fluctuation analysis of mechanochemical coupling depending on the type of biomolecular motors. *Phys. Rev. Lett.* 101, 12103 (2008).
- [95] Tsygankov, D., Serohijos, A. W. R., Dokholyan, N. V. & Elston, T. C. Kinetic models for the coordinated stepping of cytoplasmic dynein. *J. Chem. Phys.* 130, 025101 (2009).
- [96] Tsygankov, D., Serohijos, A. W. R., Dokholyan, N. V. & Elston, T. C. A physical model reveals the mechanochemistry responsible for dynein's processive motion. *Biophys. J.* 101, 144-150 (2011).
- [97] Swierczek, M., Cieluch, E., Sarewicz, M., Borek, A., Moser, C. C., Dutton, P. L. & Osyczka, A. An electronic bus bar lies in the core of cytochrome bc1. *Science* 329, 451-454 (2010).
- [98] Sarewicz, M. & Osyczka, A. Electronic connection between the quinone and cytochrome c redox pools and its role in regulation of mitochondrial electron transport and redox signaling. *Physiol. Rev.* 95, 219-243 (2015).
- [99] Iversen, L., Tu, H.-L., Lin, W.-C., Christensen, S. M., Abel, S. M., Iwig, J. & et al. Ras activation by SOS: Allosteric regulation by altered fluctuation dynamics. *Science* 345, 50-54 (2014).
- [100] Nakamura, Y., Hibino, K., Yanagida, T. & Sako, Y. Switching of the positive feedback for Ras activation by a concerted function of SOS membrane association domains. *Biophys. Physbiol.* 13, 1-11 (2016).
- [101] Crutchfield, J. P. Between order and chaos, *Nature Phys.* 8, 17-24 (2012).
- [102] Penrose, O. *Foundations of Statistical Mechanics. A Deductive Treatment.* (Pergamon Press, Oxford, 1970).
- [103] Anderson, P. W. More is different. *Science* 177, 393-396 (1972).
- [104] Zurek, W. H. Decoherence, einselection, and the quantum origins of the classical. *Revs Mod. Phys.* 75, 715-765 (2003).
- [105] Zurek, W. H. Quantum Darwinism. *Nature Phys.* 5, 181-188 (2009).
- [106] Eldredge, N. & Gould, S. J. (1972). Punctuated equilibria: an alternative to phyletic gradualism. in Schopf, T. J. M., ed. *Models in Paleobiology*, pp. 82-115 (Freeman, San Francisco, 1972).
- [107] Bak, P. & Sneppen, K. Punctuated equilibrium and criticality in simple model of evolution. *Phys Rev. Lett* 71, 4083-4086 (1993).